Original Article
Silencing miR-454 suppresses cell proliferation, migration and invasion via directly targeting MECP2 in renal cell carcinoma

Huan Liu[1], Qun-Long Liu[2], Ting-Shuai Zhai[1], Jun Lu[1], Yun-Ze Dong[1], Yun-Fei Xu[1]

[1]Department of Urology, Shanghai Tenth People's Hospital, School of Medicine in Tongji University, Shanghai 200072, China; [2]Department of Urology, Shanghai Tenth People's Hospital, Nanjing Medical University, Nanjing 210029, China

Abstract: Renal cell cancer (RCC) is one of the most common malignant tumors of the urinary system. MicroR-NA-454 (miR-454) has been reported to play an important role in various cancer progressions, such as hepatocellular carcinoma, breast cancer and glioblastoma. Nevertheless, its effect on RCC still remains unknown. We aimed to investigate the biological function and underlying mechanisms of miR-454 in RCC. The expressions of miR-454 and MECP2 in RCC tissues were assessed using data from TCGA database and our own clinical samples. Functional experiments Cell Counting Kit-8 (CCK-8), colony formation, wound healing and Transwell assays were applied to detect the effects of miR-454 and MECP2 in RCC. The interaction between miR-454 and MECP2 was assessed by western blot and luciferase reporter assays. MiR-454 was upregulated in RCC tissues and cell lines compared with matched adjacent normal tissues and the normal kidney tubular epithelial cell line HK-2. MiR-454 inhibition and methyl-CpG binding protein 2 (MECP2) overexpression could both decrease the proliferative, migrative and invasive abilities of RCC cells. Higher expression of miR-454 predicted a poor overall survival (OS) (HR: 1.8; P < 0.05), while MECP2 level was positively related with RCC OS (HR: 0.55; P < 0.05) and disease-free survival (HR: 0.56; P < 0.05). Mechanistically, we showed that miR-454 could directly target the downstream gene *MECP2*. Our findings indicated that miR-454 accelerates RCC progression via suppressing *MECP2* expression, which may provide a novel potential target of RCC treatment in the future.

Keywords: miR-454, oncogene, MECP2, renal cell cancer

Introduction

Renal cell cancer (RCC) is one of the most common malignant tumors of the urinary system, accounting for approximately 4% (65,340 cases) of newly diagnosed carcinomas and 2% (14,970) of cancer deaths in the United States in 2018 [1]. For localized or early stage RCC, the best treatment is surgical resection (partial or radical nephrectomy), which has a 92.6% 5-year survival rate [2]. However, for metastatic RCC, the 5-year survival rate is very poor due to its resistance to radiotherapy and chemotherapy [3]. Although tyrosine kinase inhibitor (TKI)-based antiangiogenic drugs have improved the prognosis of RCC, most patients will still experience tumor progression and ultimately die due to drug resistance [4]. Thus, it is extremely important to uncover the underlying mechanisms of RCC and identify additional prognostic biomarkers and therapeutic targets for RCC.

MicroRNAs (miRs) are a class of small [19-22 nt (nucleotides) in length] non-coding RNAs, which can regulate the expression of target genes through binding to the 3'-untranslated (3'-UTR) region thus causing degradation or inhibition of translation of the mRNAs [5]. In recent years, various miRNAs have been identified with the development of high-throughput sequencing and bioinformatics use, and they have been widely shown to play an important role in tumor occurrence. Among them, miR-454 has been reported to regulate cancer development by acting as an oncogene or tumor suppressor in tumorigenesis. For example, Zhu found that

miR-454 was overexpressed in hepatocellular carcinoma (HCC) cell lines and tissues, and upregulating miR-454 could promote proliferation, invasion, and epithelial/mesenchymal transition (EMT) processes in HCC [6]. Song reported that overexpressing miR-454 in triple-negative breast cancer cells could decrease VGLL4 levels and promote tumor cell growth [7]. Conversely, in osteosarcoma and glioblastoma, miR-454 suppressed cancer cell proliferation and invasion [8, 9]. However, until now, the roles and underlying molecular mechanisms of miR-454 in RCC development still remain unknown and need to be elucidated.

Thus, in the present study we aimed to describe the effect of miR-454 in RCC and we found that miR-454 was overexpressed in RCC tissues based on The Cancer Genome Atlas (TCGA) database and analyses of clinical tumor specimens. Silencing miR-454 inhibited the proliferation, invasion, and migration of RCC cells. Furthermore, we found that methyl-CpG binding protein 2 (MECP2) was the direct downstream target of miR-454. Our findings suggest an oncogenic role for miR-454 in RCC and may provide a novel potential target for RCC therapy.

Materials and methods

RCC tissue samples

Nineteen clear cell RCC (ccRCC) samples and paired adjacent normal tissue specimens were collected from Shanghai Tenth People's Hospital between January 2017 and June 2019. The fresh tumor tissues were kept in liquid nitrogen to avoid the degradation of RNA. All tissue specimen use was evaluated and approved by the Ethical Committees of Shanghai Tenth People's Hospital of Tongji University. All patients provided written informed consent.

Bioinformatics analysis

The expression of miR-454 and MECP2 was evaluated based on The Cancer Genome Atlas Program (TCGA) kidney Clear Cell Carcinoma (KIRC) database (https://www.cancer.gov/). The potential target genes of miR-454 were predicted using TargetScan (http://www.targetscan.org/), miRDB (http://mirdb.org/), and miDIP (http://ophid.utoronto.ca/mirDIP/).

Cell lines and culture

Human ccRCC cell lines OSRC-2, SN12-PM6, ACHN, and SW839, and human normal kidney tubular epithelial cell line HK-2 were purchased from Cell Bank of the Chinese Academy of Sciences (Shanghai, China). HK-2 cells were cultured in Keratinocyte Medium (KM, ScienCell, San Diego, USA) plus 1% Keratinocyte Growth Supplement (KGS, ScienCell, San Diego, USA) and the other RCC cells and HEK293T cells (human embryonic kidney cells) were cultured in Dulbecco's Modified Eagle's Medium (DMEM, Gibco, USA) plus 10% fetal bovine serum (FBS; Hyclone, Logan, Utah, USA). Both the culture media were added with 1% penicillin/streptomycin (P/S; Gibco, New York, NY, USA). All cells were cultured in a humidified atmosphere at 37° with 5% CO_2.

RNA extraction, reverse transcription and quantitative real-time PCR analyses (qRT-PCR)

Total RNA was extracted from cultured cells and human frozen tissues using Trizol reagent (Invitrogen, Carlsbad, CA, USA) according to the manufacturer's instructions. A Nanodrop 2000 spectrophotometer (Thermo Fisher Scientific, San Jose, CA, USA) was used to assess the purity and concentration of RNA. Reverse transcription was performed to synthesize the cDNA with a PrimeScript RT reagent kit (TaKaRa, Japan). The qRT-PCR was performed using a SYBR Green qPCR Kit (Takara, Japan) and the ABI Prism 7500 Detection System (Applied Biosystems, San Jose, CA, USA). The expressions of miR-454 and MECP2 were normalized to GAPDH or U6 applying the $2^{-\Delta\Delta Ct}$ method. The primer details are as follow: miR-454 reverse transcribed primer: 5'-GTCGTATCCAGTGCAGG-GTCCGAGGTATTCGCACTGGATACGACACCCTA-3'; miR-454 forward: 5'-ACCCTATCAATATTGT-CTCTGC-3'; miR-454 reverse: 5'-TGGTGTCGTG-GAGTCG-3'; U6 reverse transcribed primer: 5'-CGCTTCACGAATTTGCGTGTCAT-3'; U6 forward: 5'-CTCGCTTCGGCAGCACA-3'; U6 reverse: 5'-AACGCTTCACGAATTTGCGT-3'; MECP2 forward: 5'-AACGCTTCACGAATTTGCGT-3'; MECP2 reverse: 5'-AGGCGAAGGCGGCTCCAG-3'; GAPDH forward: 5'-CAATGACCCCTTCATTGACC-3'; and GAPDH reverse: 5'-TTGATTTTGGAGGGA-TCTCG-3'.

Western blot analysis

Cells were lysed on ice using RIPA buffer (Beyotime, Shanghai, China) containing protease inhibitors. Equal amounts (30 µg) of protein samples was loaded onto 10% sodium dodecyl sulfate-polyacrylamide gel electrophoresis gels and then transferred to polyvinylidene fluoride membranes. The membranes were blocked in 5% skim milk and then incubated overnight at 4°C with primary antibodies as follows: anti-MECP2 (1:1000; ABclonal, Wuhan, China), and anti-GAPDH (1:5000; Abcam, Cambridge, UK). Next, the membranes were incubated with secondary rabbit antibody (1:1000; ABclonal, Wuhan, China) for 1 h at room temperature. After washing three times in PBST, the fluorescence was scanned by the Odyssey scanner (LI-COR Biosciences, Lincoln, NE, USA).

Cell proliferation assays

The Cell Counting Kit-8 (CCK-8, Dojindo, China) was applied to measure cell proliferation according to the manufacturer's protocol. Briefly, $1×10^3$ per well transfected RCC cells were seeded into 96-well plates and cultured for 24-120 h. Every 24 h, we measured the optical density (OD) value using an auto-microplate reader (BioTek Solutions, Thousand Oaks, CA, USA), after incubating for 2 h with CCK-8 (10 µL) at 37°C in 5% CO_2.

For colony formation assays, $1×10^3$ transfected RCC cells were seeded into the 6-well plate per well and cultured in 10% FBS/DMEM for 2 weeks. Subsequently, cells were fixed in 95% ethanol and stained with 0.1% Crystal Violet solution. After removing the staining solution, colonies were imaged and counted.

Wound healing assays

For wound healing assays, cells were seeded in triplicate into 6-well plates and a wound was made using a 200 µL pipette tip on the cell monolayer after the monolayer reached 80-90% confluency. Culture media was replaced with 2% FBS/DMEM. Then, cells were incubated for additional 24 h and photographed using microscopy (Leica Microsystems, Mannheim, Germany).

Transwell assays

Transwell chambers (Corning, MA, USA) with 8-µm pore size polycarbonate filters were used to evaluate the migration and invasion of RCC cells. Cells ($5×10^4$ cells) were seeded in serum-free medium in the upper chamber, which was pre-covered with or without Matrigel (Corning, BD356230), and 600 µL 10% FBS/culture medium was added to the lower chamber. After incubation, the cells in the upper surface of the filters were removed using a cotton swab. Then we fixed the cells migrated or invaded to the lower surface of the filter using 95% ethanol for 15 min, and stained with 0.1% Crystal Violet solution for 20 min. Cell numbers were counted in five randomly chosen fields under a microscope (Leica Microsystems).

Cells transfection

MiRNA negative control (miR-NC), miR-454 mimics, and inhibitors were purchased from Ribobio (Guangzhou, China). Transient transfection with these reagents was performed using Lipofectamine 3000 according to manufacturer's protocol. For overexpressing MECP2, the MECP2 vector and overexpression (MECP2-OE) plasmids were synthesized by IBSBIO Biotech (Shanghai, China). We transfected the plasmids into HEK293T cells to package the lentivirus using the Lentivirus-Packaging kit (BioLink, Shanghai, China). After 24 h, the lentivirus supernatants were collected and used to infect cells.

Luciferase reporter assays

The binding sites of miR-454 and MECP2 were obtained from TargetScan and the psiCHECK-2 vector (Promega, Madison, WI, USA) containing wild-type (WT) or mutant-type (Mut) sequence was synthesized by BIOFAVOR Biotech (Wuhan, China). HEK293T cells were seeded in 12-well plates and co-transfected with the luciferase reporter vector (MECP2-WT or MECP2-Mut) and miR-454 mimics or control (NC). After 48 h transfection, the relative luciferase activity was measured by a Dual Luciferase Assay System kit (Promega, San Luis Obispo, CA, USA) according to the manufacturer's protocol.

Immunohistochemistry (IHC)

IHC was performed to assess the expression levels of MECP2 in tissues as described previously [10]. The samples were fixed in formalin, embedded in paraffin and then cut into 4-µm thick sections. After being dewaxed, rehydrated, and following antigen retrieval, the sec-

tions were incubated in specific primary antibody against MECP2 (ABclonal). Images were captured using a microscope (Leica Microsystems).

Statistical analysis

Statistical analyses were performed using the GraphPad Prism 8 (GraphPad Software, CA). All data were presented as the mean ± standard deviation (SD) from three independent experiments. Statistical significance between groups was analyzed using the Student's *t*-test. The correlations between miR-454 and MECP2 were tested using Pearson's correlation coefficient analysis. All data were considered statistically significant at P < 0.05.

Results

MiR-454 was upregulated in RCC tissues and cell lines and predicted poor survival

To detect the expression of miR-454 in RCC tissues, we searched the GEO dataset and identified GSE16441, which conducted miRNA expression profiling array analyses in 17 RCC tumor samples compared with matched non-tumor samples. MiR-454 was significantly upregulated in RCC samples (fold changes > 2, *p*-value < 0.05) (**Figure 1A**, **1B**). Based on TCGA KIRC database, we also observed that miR-454 was overexpressed in RCC tissues compared with un-paired or paired adjacent samples (P < 0.0001) (**Figure 1C**, **1D**), and Kaplan-Meier survival analyses indicated that high miR-454 expression was closely related with poor survival (P < 0.005) (**Figure 1E**). Additionally, we also validated the expression of miR-454 in RCC cell lines and 19 paired clinical specimens. Consistently, miR-454 was highly expressed in RCC samples and cell lines when compared with normal tissues and normal kidney tubular epithelial cell line HK-2 (**Figure 1F**, **1G**). Because OSRC-2 and SW839 showed higher expressions of miR-454, we chose these two cell lines for further studies.

Inhibiting miR-454 attenuated proliferation, migration, and invasion of RCC cells

MiR-454 inhibitors were transfected into OSRC-2 and SW839 cells and the inhibition efficiency was detected by qRT-PCR (**Figure 2A**). CCK-8 assays showed that the viability of RCC cells was attenuated after transfection with miR-454 inhibitors (**Figure 2B**). Compared with negative control (NC), the colony formation number of the miR-454 inhibitor group was decreased both in OSRC-2 and SW839 cells (**Figure 2C**). Additionally, the wound healing assay indicated that silencing miR-454 significantly suppressed cell migration in OSRC-2 and SW839 cells (**Figure 2D**). Transwell assays also revealed that the migration and invasion of RCC cells were suppressed after knockdown of miR-454 (**Figure 2E**, **2F**).

MECP2 was the downstream target of miR-454

To explore the downstream targeted genes of miR-454, we queried the TargetScan, miDIP and miRDB databases. Nineteen candidates emerged after overlapping the results from three databases (**Figure 3A**). As the above-mentioned results had shown that miR-454 acted as an oncogene in RCC, we focused on tumor suppressors among the predicted targets. Based on TCGA KIRC database, we measured the expression of 19 candidates in RCC samples (data not shown) and found that MECP2 was significantly downregulated in RCC tissues compared with normal non-paired or paired adjacent samples (**Figure 3B**). Pearson's correlation coefficient analysis also revealed that miR-454 expression level was inversely correlated with MECP2 both in TCGA KIRC and for our clinical samples (**Figure 3C**). Additionally, western blots also demonstrated that inhibition of miR-454 could increase the protein level of MECP2 (**Figure 3D**). To further verify that miR-454 targeted MECP2, we found a putative binding site of miR-454 in the 3'-UTR of MECP2 and inserted the luciferase reporter with wild-type or mutant sequences (**Figure 3E**). The results showed that the relative luciferase activity was apparently decreased by miR-454 mimics in HEK293T cells transfected with wild-type constructs, while no significant difference was observed in the mutant group (**Figure 3F**). Taken together, the above results implied that MECP2 was the direct target of miR-454.
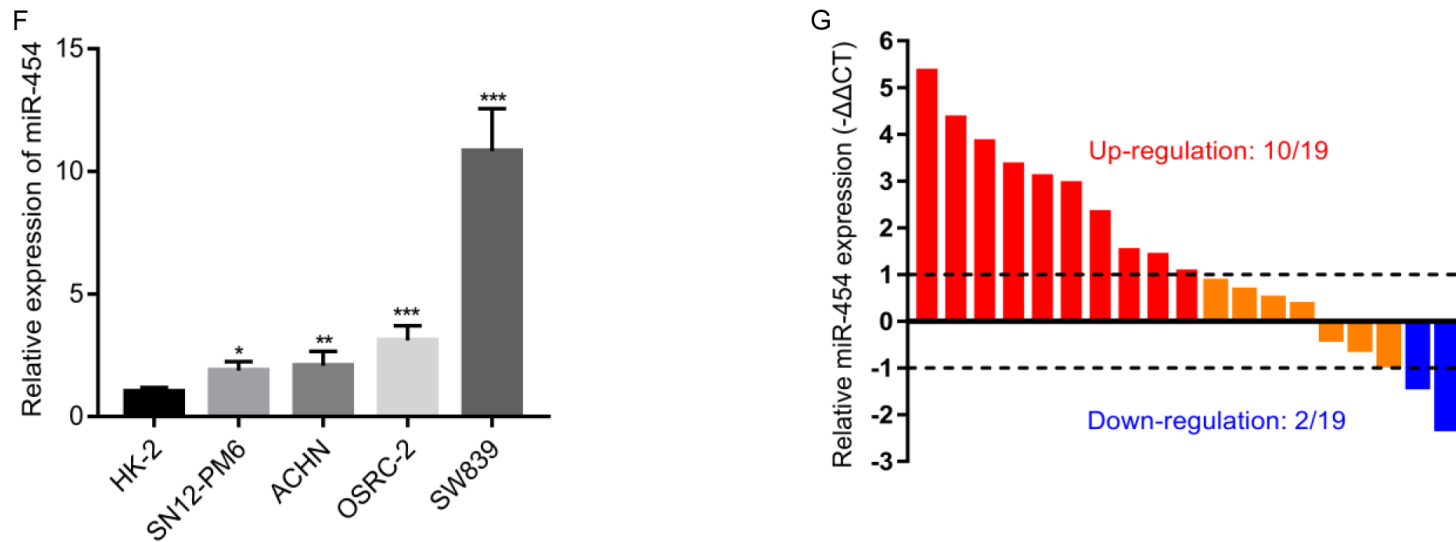
MECP2 had low expression in RCC cell lines and tissues

Western blotting and qRT-PCR were applied to assess the expression of MECP2 in RCC cell
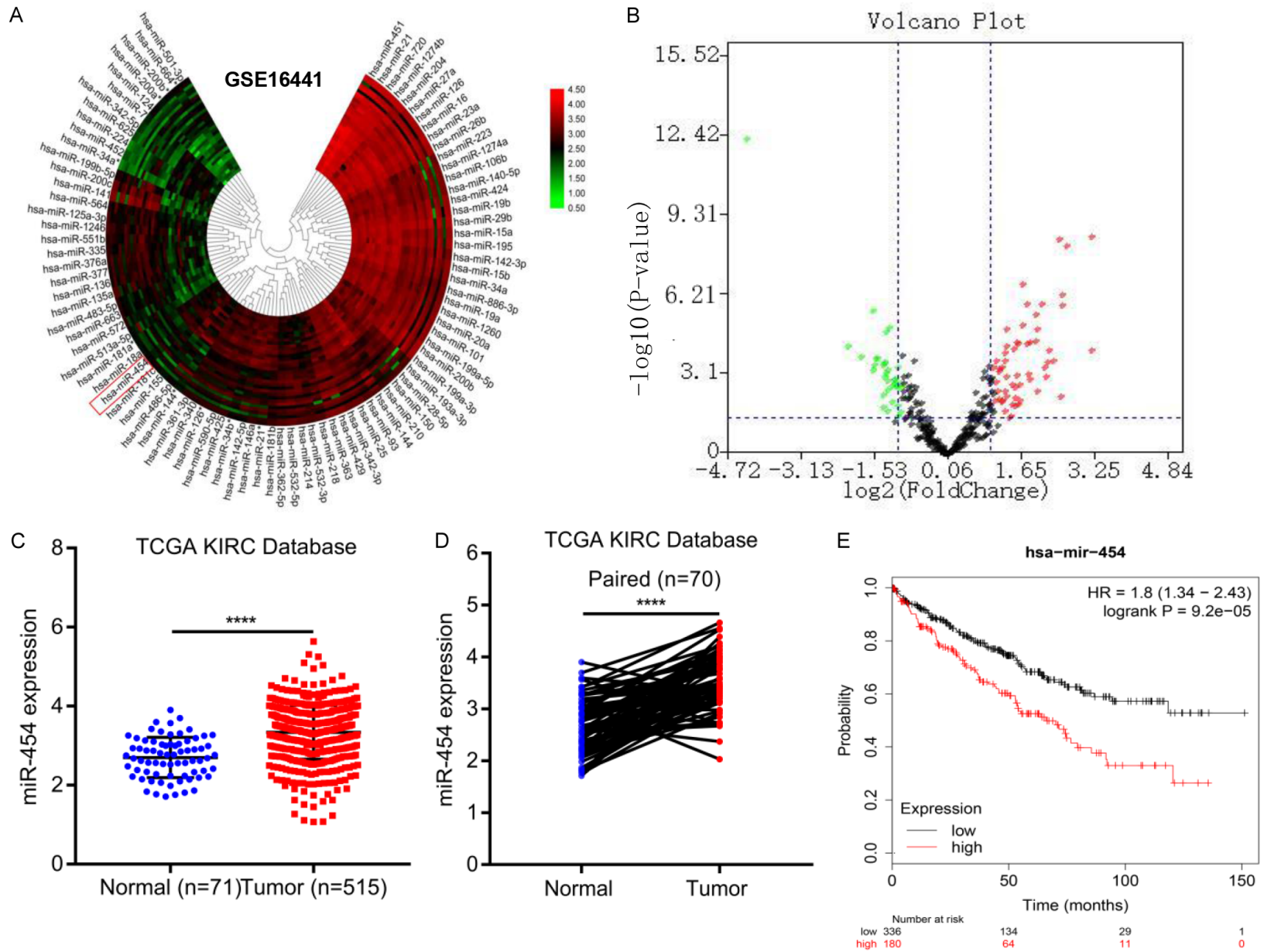
Figure 1. MiR-454 is significantly up-regulated in RCC tissues and cells, and predicts a poor survival of RCC. A and B. Expression level of miR-454 in the miRNA expression profiling array was presented by clustered heatmap and volcano plot. C and D. Expression of miR-454 in un-paired and paired RCC tissues based on TCGA database. E. Kaplan-Meier survival analysis of miR-454 expression on the overall survival of RCC patients. F. Relative expression of miR-454 in four RCC cell lines (OSRC-2, SN12-PM6, ACHN, SW839) compared with human normal kidney tubular epithelial cell line HK-2. G. Relative expression of miR-454 in our 19 clinical RCC tissues and matched adjacent normal specimens ($*P < 0.05$, $**P < 0.01$, $***P < 0.001$, $****P < 0.0001$).
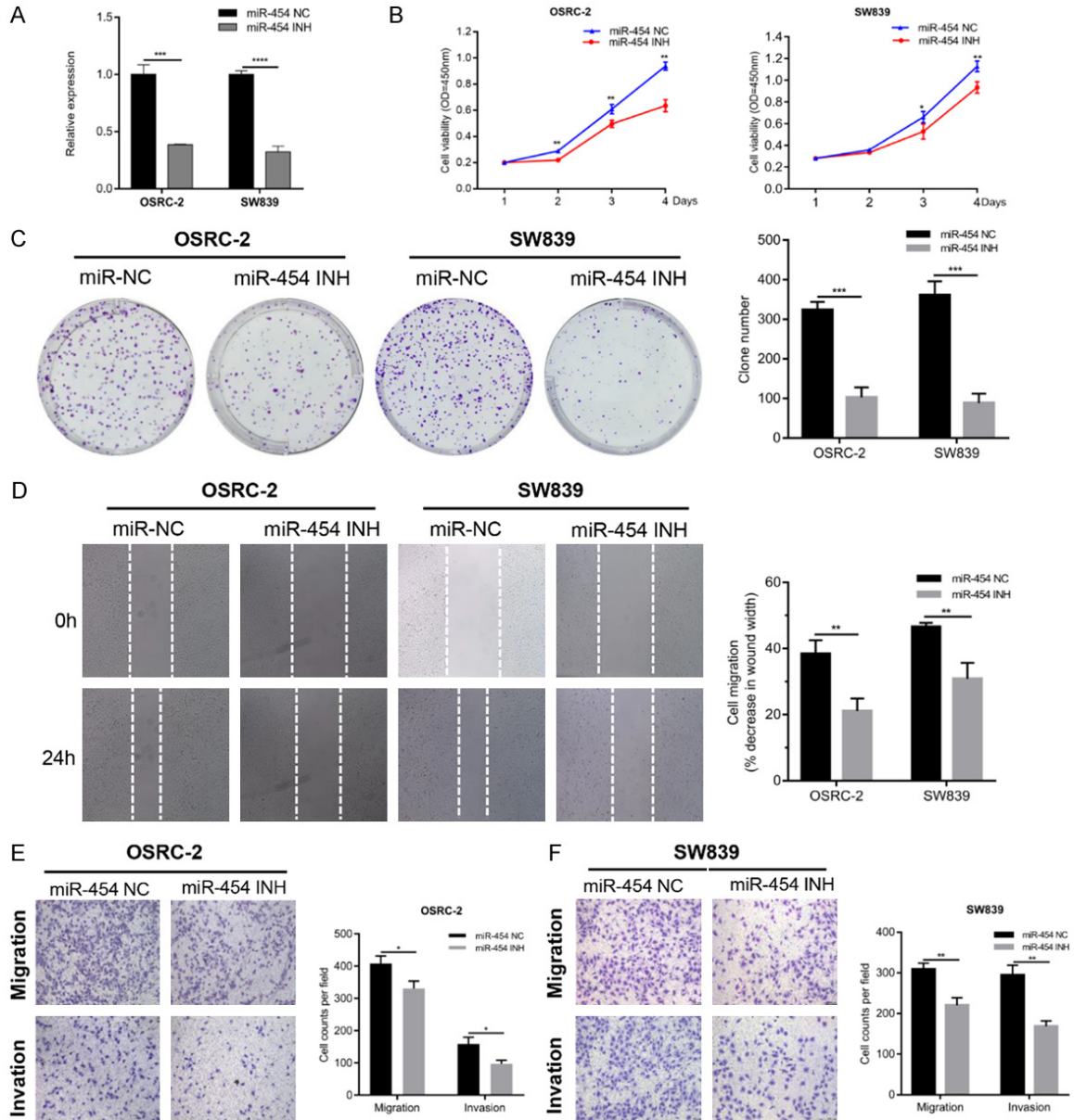
Figure 2. Inhibition of miR-454 suppresses proliferation, migration and invasion of RCC cells. A. The expression of miR-454 was detected by qRT-PCR in RCC cells transfected with miR-454 inhibitor or NC. B. CCK-8 assay of RCC cells after transfection with miR-454 inhibitor or NC. C. Colony formation assay of RCC cells after transfection with miR-454 inhibitor or NC. D. Wound healing analysis of RCC cells after transfection with miR-454 inhibitor or NC. E and F. Transwell assays of RCC cells after transfection with miR-454 inhibitor or NC. Data indicate mean ± SD of three experiments (*P < 0.05, **P < 0.01, ***P < 0.001, ****P < 0.0001).

lines and tissues. The results showed that MECP2 was downregulated in RCC cell lines compared with HK-2 cells both in mRNA and protein levels (**Figure 4A**, **4B**). Consistent with the abovementioned TCGA data (**Figure 3B**), our clinical samples also showed that MECP2 had low expression levels in RCC tissues (**Figure 4C**). Moreover, we also performed immunohisto-

chemical analyses in RCC tissues and matched adjacent normal specimens, and found MECP2 expression was significantly decreased in tumor tissues (**Figure 4D**). In addition, the Kaplan-Meier survival analysis based on TCGA indicated that patients with higher MECP2 expression in KIRC had significantly longer overall survival (OS) and disease-free survival (DFS) rates
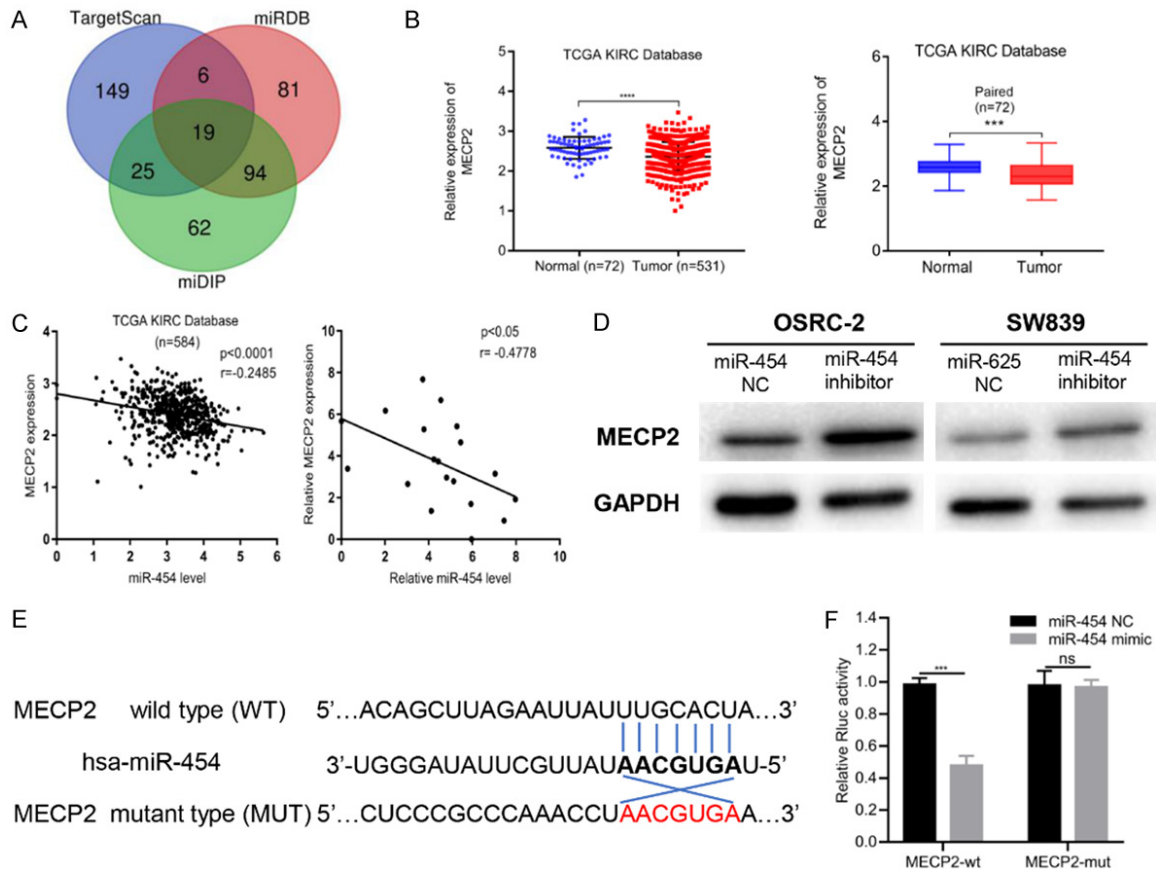
Figure 3. MiR-454 directly targets downstream gene MECP2. A. The diagram of miR-454 potential target genes predicted by TargetScan, miDIP and miRDB databases. B. Relative expression of MECP2 in un-paired or paired RCC tissues based on TCGA database. C. The expression of MECP2 was inversely correlated with miR-454 level in TCGA KIRC and our clinical samples. D. MECP2 protein level was assessed by western blot after transfecting miR-454 mimics or NC into RCC cells. E. Schematic of MECP2 wild-type (WT) and mutant (Mut) luciferase reporter vectors. F. Relative luciferase activity measured by luciferase assays in HEK293T cells co-transfected with miR-454 mimics or NC. Data indicate mean ± SD of three experiments (*$P < 0.05$, **$P < 0.01$, ***$P < 0.001$, ****$P < 0.0001$).

(**Figure 4E**), which also suggested that MECP2 may function as a tumor suppressor in RCC.

Overexpressing MECP2 attenuated proliferation, migration, and invasion of RCC cells

OSRC-2 and SW839 cells were infected with MECP2 overexpressed lentivirus and the efficacy was validated by qRT-PCR and western blots (**Figure 5A**, **5B**). We observed that upregulation of MECP2 in RCC cells significantly inhibited cell proliferation and colony formation (**Figure 5C**, **5D**). Additionally, the wound healing and Transwell assays also showed that overexpression of MECP2 suppressed the migration and invasion abilities of RCC cells (**Figure 5E-G**). These results indicated that MECP2 exerted anti-tumor effects conversely with miR-454 in RCC cells.

MECP2 restoration reversed the effects of miR-454 in RCC cells

Rescue experiments were conducted to further validate that miR-454 promoted RCC proliferation, migration, and invasion via targeting MECP2. The RCC cells were co-transfected with miR-454 mimics or NC and MECP2 overexpressed plasmid. We observed that miR-454 mimics could promote proliferation, migration, and invasion in RCC cells and these effects were partially attenuated by MECP2 restoration (**Figure 6A-D**). In addition, miR-454 mimics decreased the protein level of MECP2 while the effect was also reversed after transfection with MECP2-overexpression plasmid (**Figure 6E**). The above results indicated that miR-454 promoted the malignant progression of RCC through repressing MECP2 expression.
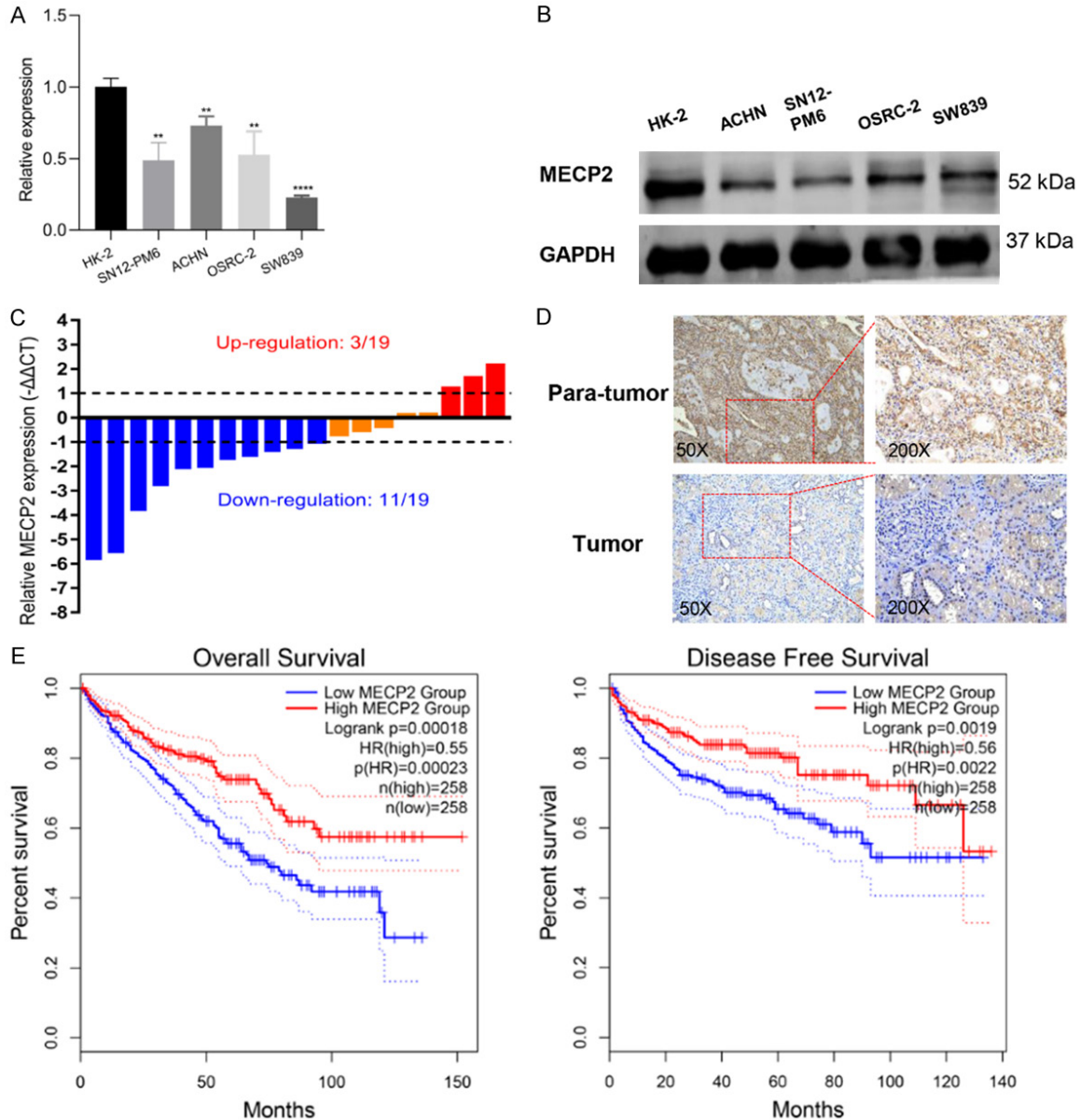
Figure 4. MECP2 is lowly expressed in RCC tissues and cells. A and B. The expression of MECP2 in four RCC cell lines (OSRC-2, SN12-PM6, ACHN, SW839) and human normal kidney tubular epithelial cell line HK-2 was measured by qRT-PCR and western blot. C. The expression of miR-454 in 19 paired RCC samples. D. Immunochemical staining of MECP2 in RCC tissues and adjacent normal tissues. E. Kaplan-Meier survival analysis of MECP2 expression on the overall and disease-free survival of RCC patients based on TCGA database ($*P < 0.05$, $**P < 0.01$, $***P < 0.001$, $****P < 0.0001$).

Discussion

Currently, studies have demonstrated that miR-NAs are closely associated with RCC occurrence [11-14]. However, as far as we know, the expression level and function of miR-454 in RCC still remain unknown. In this study, we found that miR-454 was highly expressed in RCC cell lines and tumor tissues, which was consistent with data from TCGA KIRC database. Moreover, the results from miRNA expression profiling arrays (GSE16441) also showed that miR-454 was significantly upregulated in RCC tumor specimens.

To date, miR-454 has been widely reported in other tumors, but its role in tumorigenesis is controversial. In osteosarcoma, miR-454 was
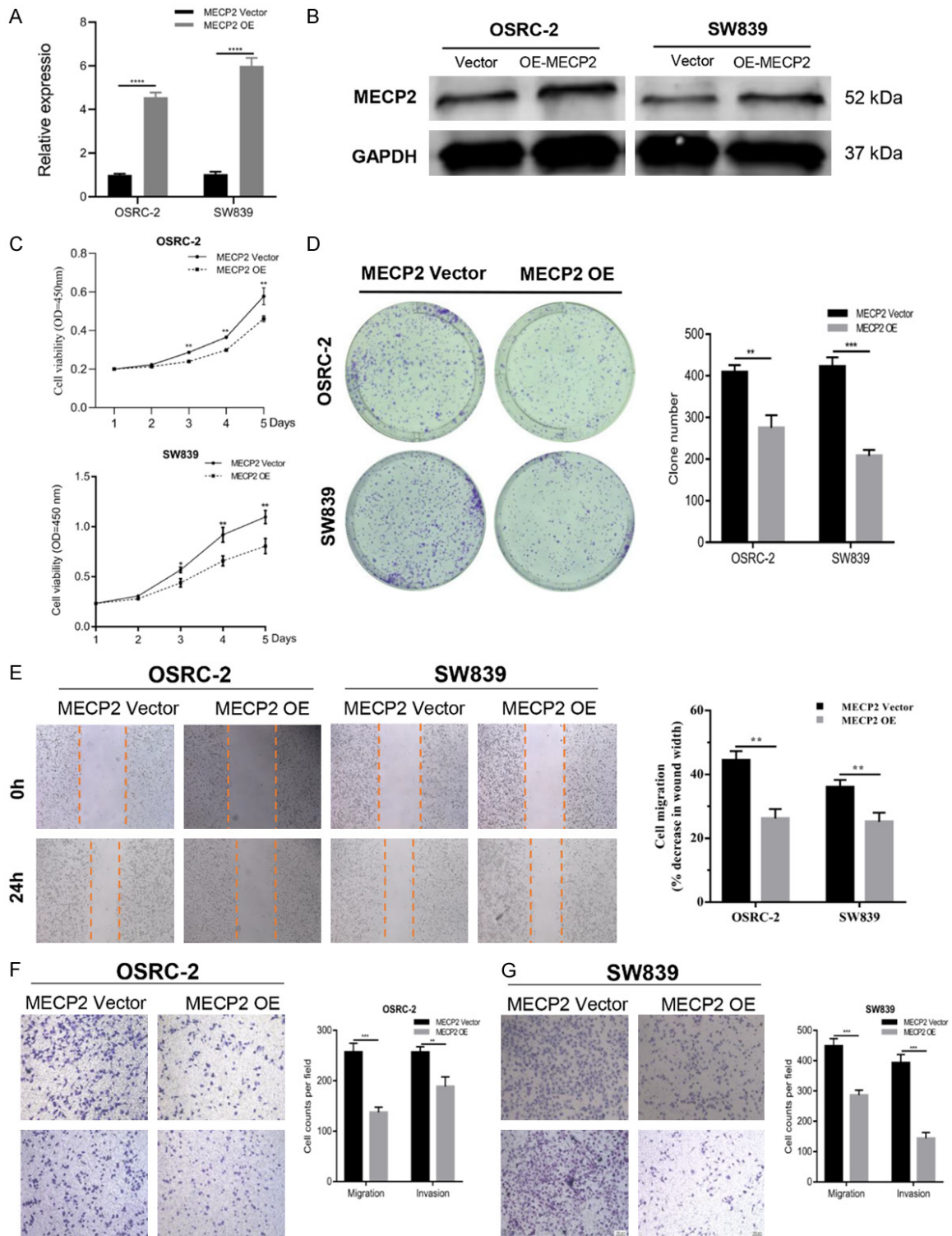
Figure 5. MECP2 inhibits the proliferation, migration and invasion capacity of RCC cells. A and B. The efficacy of MECP2 overexpressed plasmid was validated by qRT-PCR and western blot. C-G. CCK-8, colony formation, wound healing and transwell assays of RCC cells after transfection with MECP2 overexpressed plasmid or vector. Data indicate mean ± SD of three experiments (*P < 0.05, **P < 0.01, ***P < 0.001).

downregulated in tumor tissues and cell lines and inhibited tumor growth and invasion through targeting c-Met [9]. Likewise, miR-454 was also reported to act as a tumor-suppressor
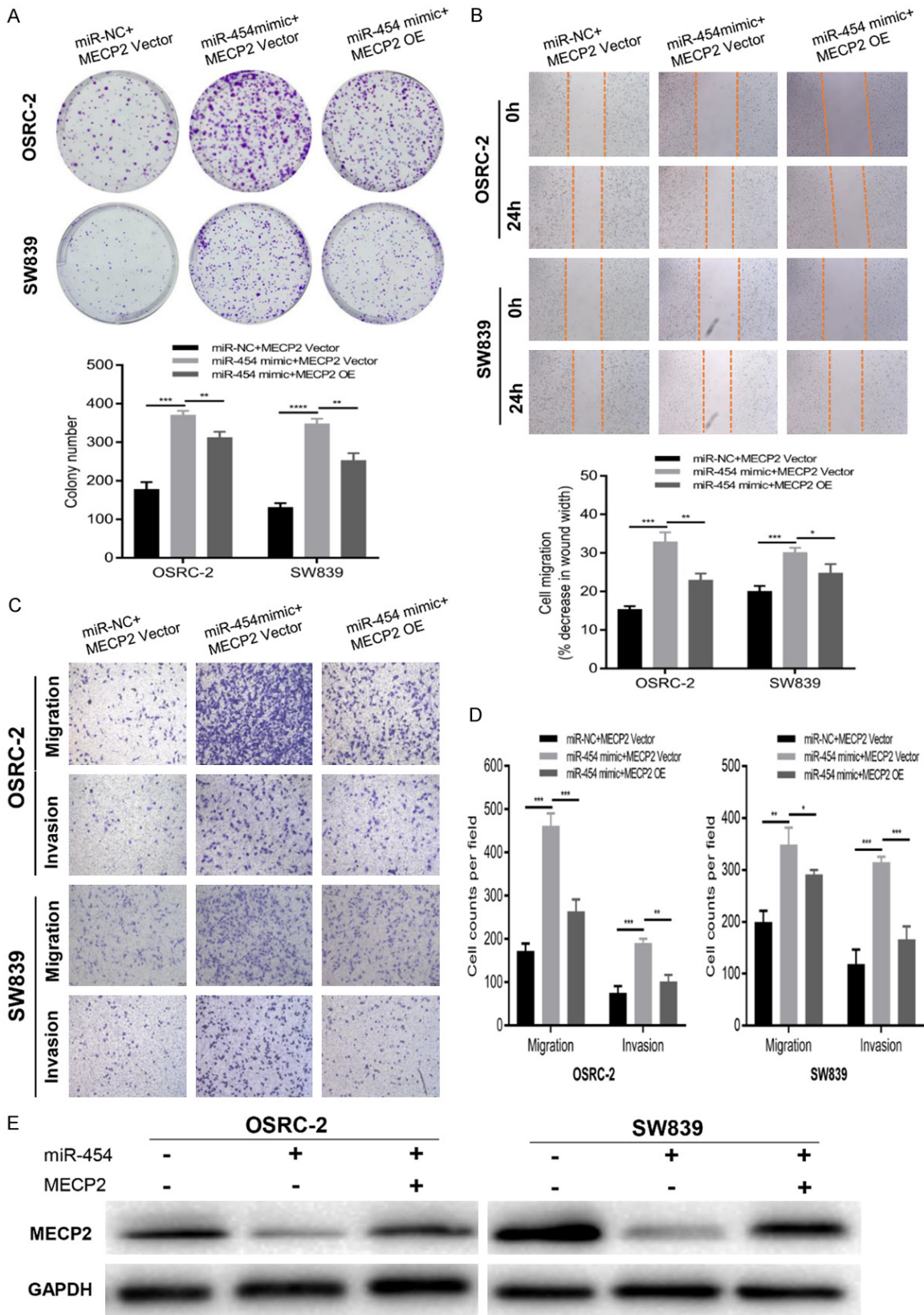
Figure 6. MECP2 restoration reverses the effect of miR-454 in RCC cells. A-D. Colony formation, wound healing and transwell assays of RCC cells co-transfected with miR-454 mimics and MECP2 overexpressed plasmids. E. The protein level of MECP2 in RCC cells co-transfected with miR-454 mimics and MECP2 overexpressed plasmids. Data indicate mean ± SD of three experiments (*$P < 0.05$, **$P < 0.01$, ***$P < 0.001$).

to inhibit proliferation of glioblastoma cells by suppressing the expression of PDK1 [8]. However, contrary effects of miR-454 were observed in HCC and prostate cancer [6, 15]. Yu et al. reported that knockdown of miR-454 impeded cell proliferation and invasion and EMT in HCC, whereas miR-454 overexpression could induce HCC cell proliferation, invasion, and EMT [6]. Li found that miR-454 was overexpressed in prostate cancer samples and cell lines and the functional experiments suggested that miR-454 played an oncogenic role in promoting prostate cancer cell proliferation and invasion via downregulation of NDRG2 [15].

In the present study, we observed that the proliferation, migration, and invasion of RCC cells were suppressed after knockdown of miR-454, whereas overexpressing miR-454 increased proliferation, migration, and invasion of RCC cells. Additionally, Kaplan-Meier survival analyses showed that higher miR-454 expression indicated a poorer survival, which also revealed that miR-454 exerted a tumor promoting effect on RCC. Previous study has reported that Von Hippel-Lindau tumor suppressor (VHL) could alter the expression of miRNA [16]. Interestingly, in our study, we observed that miR-454 was relatively highly expressed in VHL-mutated RCC cell lines (OSRC-2 and SW839) compared with VHL wild-type cells (SN12-PM6). The expression of miR-454 may be related with VHL status, which should be investigated further.

The interaction between miR-454 and its target gene was predicted by commonly used online tools. The luciferase reporter analysis demonstrated that miR-454 could directly target MECP2 through binding to the 3'-UTR and repressing translation of MECP2 mRNA, which was consistent with the results of western blots. Pearson's correlation coefficient analysis also revealed that miR-454 expression level was negatively correlated with MECP2 in RCC tissues.

MECP2 is a key epigenetic regulator which binds to methylated DNA or gene promoters to regulate gene transcription and chromatin organization [17, 18]. MECP2 has been well studied in neuronal systems and its mutations are the main cause of the neurological disorder Rett syndrome and mental retardation in females [19, 20]. Recently, MECP2 was report-

ed to play an important role in malignancy [21-24]. For instance, Chen et al. showed that MECP2 was highly expressed in gastric cancer (GC) tissues and induced proliferation of GC cells through a FOXF1-regulated Wnt5a/β-Catenin signaling pathway [21]. In glioma, MECP2 was reported to exert a tumor suppressive effect on proliferation, migration, invasion, and adhesion of glioma cells. Overexpression of MECP2 leads to decreased p-ERK and BDNF expression while increasing GFAP expression in glioma cells [22]. As far as we know, the role of MECP2 in RCC has not been previously studied. Here, we first reported the expression and effects of MECP2 in RCC tissues and cell lines. We observed that MECP2 was downregulated in RCC cell lines and tissues, based on TCGA database and data from our clinical samples. Overexpressing MECP2 could decrease the biological function of RCC cells.

In summary, our results revealed that miR-454 was highly expressed in tumor tissues and acted as an oncogene to promote the progression of RCC through targeting MECP2, which perhaps may provide a new therapeutic target for RCC.

Acknowledgements

Disclosure of conflict of interest

None.

Address correspondence to: Yun-Fei Xu, Department of Urology, Shanghai Tenth People's Hospital, School of Medicine in Tongji University, Shanghai 200072, China. E-mail: 1811375@tongji.edu.cn

References

[1] Bray F, Ferlay J, Soerjomataram I, Siegel RL, Torre LA and Jemal A. Global cancer statistics 2018: GLOBOCAN estimates of incidence and mortality worldwide for 36 cancers in 185 countries. CA Cancer J Clin 2018; 68: 394-424.

[2] Patard JJ, Pignot G, Escudier B, Eisen T, Bex A, Sternberg C, Rini B, Roigas J, Choueiri T, Bukowski R, Motzer R, Kirkali Z, Mulders P and

Bellmunt J. ICUD-EAU international consultation on Kidney cancer 2010: treatment of metastatic disease. Eur Urol 2011; 60: 684-690.

[3] Zhai W, Ma J, Zhu R, Xu C, Zhang J, Chen Y, Chen Z, Gong D, Zheng J, Chen C, Li S, Li B, Huang Y, Xue W and Zheng J. MiR-532-5p suppresses renal cancer cell proliferation by disrupting the ETS1-mediated positive feedback loop with the KRAS-NAP1L1/P-ERK axis. Br J Cancer 2018; 119: 591-604.

[4] van der Mijn JC, Mier JW, Broxterman HJ and Verheul HM. Predictive biomarkers in renal cell cancer: insights in drug resistance mechanisms. Drug Resist Updat 2014; 17: 77-88.

[5] Chai B, Guo Y, Cui X, Liu J, Suo Y, Dou Z and Li N. MiR-223-3p promotes the proliferation, invasion and migration of colon cancer cells by negative regulating PRDM1. Am J Transl Res 2019; 11: 4516-4523.

[6] Yu L, Gong X, Sun L, Yao H, Lu B and Zhu L. miR-454 functions as an oncogene by inhibiting CHD5 in hepatocellular carcinoma. Oncotarget 2015; 6: 39225-39234.

[7] Song H, Luo Q, Deng X, Ji C, Li D, Munankarmy A, Jian W, Zhao J and Fang L. VGLL4 interacts with STAT3 to function as a tumor suppressor in triple-negative breast cancer. Exp Mol Med 2019; 51: 141.

[8] Fang B, Zhu J, Wang Y, Geng F and Li G. MiR-454 inhibited cell proliferation of human glioblastoma cells by suppressing PDK1 expression. Biomed Pharmacother 2015; 75: 148-152.

[9] Niu G, Li B, Sun J and Sun L. miR-454 is downregulated in osteosarcomas and suppresses cell proliferation and invasion by directly targeting c-Met. Cell Prolif 2015; 48: 348-355.

[10] Zhai W, Zhu R, Ma J, Gong D, Zhang H, Zhang J, Chen Y, Huang Y, Zheng J and Xue W. A positive feed-forward loop between LncRNA-UR-RCC and EGFL7/P-AKT/FOXO3 signaling promotes proliferation and metastasis of clear cell renal cell carcinoma. Mol Cancer 2019; 18: 81.

[11] Fan B, Jin Y, Zhang H, Zhao R, Sun M, Sun M, Yuan X, Wang W, Wang X, Chen Z, Liu W, Yu N, Wang Q, Liu T and Li X. MicroRNA21 contributes to renal cell carcinoma cell invasiveness and angiogenesis via the PDCD4/cJun (AP1) signalling pathway. Int J Oncol 2020; 56: 178-192.

[12] Su Z, Jiang G, Chen J, Liu X, Zhao H, Fang Z, He Y, Jiang X and Xu G. MicroRNA-429 inhibits cancer cell proliferation and migration by targeting AKT1 in renal cell carcinoma. Mol Clin Oncol 2020; 12: 75-80.

[13] Xiao W, Wang C, Chen K, Wang T, Xing J, Zhang X and Wang X. MiR-765 functions as a tumour suppressor and eliminates lipids in clear cell renal cell carcinoma by downregulating PLP2. EBioMedicine 2020; 51: 102622.

[14] Huang J, Wang X, Wen G and Ren Y. miR-NA2055p functions as a tumor suppressor by negatively regulating VEGFA and PI3K/Akt/mTOR signaling in renal carcinoma cells. Oncol Rep 2019; 42: 1677-1688.

[15] Fu Q, Gao Y, Yang F, Mao T, Sun Z, Wang H, Song B and Li X. Suppression of microRNA-454 impedes the proliferation and invasion of prostate cancer cells by promoting N-myc downstream-regulated gene 2 and inhibiting WNT/beta-catenin signaling. Biomed Pharmacother 2018; 97: 120-127.

[16] Lei Z, Klasson TD, Brandt MM, van de Hoek G, Logister I, Cheng C, Doevendans PA, Sluijter JPG and Giles RH. Control of angiogenesis via a VHL/miR-212/132 axis. Cells 2020; 9: 1017.

[17] Gadalla KK, Bailey ME and Cobb SR. MeCP2 and Rett syndrome: reversibility and potential avenues for therapy. Biochem J 2011; 439: 1-14.

[18] Yasui DH, Peddada S, Bieda MC, Vallero RO, Hogart A, Nagarajan RP, Thatcher KN, Farnham PJ and Lasalle JM. Integrated epigenomic analyses of neuronal MeCP2 reveal a role for long-range interaction with active genes. Proc Natl Acad Sci U S A 2007; 104: 19416-19421.

[19] Meehan RR, Lewis JD and Bird AP. Characterization of MeCP2, a vertebrate DNA binding protein with affinity for methylated DNA. Nucleic Acids Res 1992; 20: 5085-5092.

[20] Amir RE, Van den Veyver IB, Wan M, Tran CQ, Francke U and Zoghbi HY. Rett syndrome is caused by mutations in X-linked MECP2, encoding methyl-CpG-binding protein 2. Nat Genet 1999; 23: 185-188.

[21] Zhao L, Liu Y, Tong D, Qin Y, Yang J, Xue M, Du N, Liu L, Guo B, Hou N, Han J, Liu S, Liu N, Zhao X, Wang L, Chen Y and Huang C. MeCP2 promotes gastric cancer progression through regulating FOXF1/Wnt5a/beta-catenin and MYOD1/Caspase-3 signaling pathways. EBioMedicine 2017; 16: 87-100.

[22] Sharma K, Singh J, Frost EE and Pillai PP. MeCP2 overexpression inhibits proliferation, migration and invasion of C6 glioma by modulating ERK signaling and gene expression. Neurosci Lett 2018; 674: 42-48.

[23] Pan ZX, Zhang XY, Chen SR and Li CZ. Upregulated exosomal miR-221/222 promotes cervical cancer via repressing methyl-CpG-binding domain protein 2. Eur Rev Med Pharmacol Sci 2019; 23: 3645-3653.

[24] Song N, Li K, Wang Y, Chen Z and Shi L. Lentivirusmediated knockdown of MeCP2 inhibits the growth of colorectal cancer cells in vitro. Mol Med Rep 2016; 13: 860-866.